ADVANCES IN THE PROGRESSIVE DAMAGE ANALYSIS OF COMPOSITES

M. Bruyneel, J.P. Delsemme, P. Jetteur (LMS Samtech, Belgium);
A.C. Goupil (ISMANS, France).

Dr. Ir. M. Bruyneel, R&D Team Manager

THEME

Composites.

SUMMARY

Recent results obtained in the modelling of inter and intra-laminar damages with the SAMCEF finite element code are presented. The progressive damage models available in SAMCEF are the Cahan models. A specific model available in SAMCEF can be used to study the progressive damage inside the ply, accounting for fibres breaking, matrix cracking and fibre-matrix de-cohesion. On the other hand, delamination can also be studied with the cohesive elements approach. These models are based on the continuum damage mechanics, and damage variables impacting the stiffness of the ply or of the interface are associated to the different failure modes. A new non local model has been developed recently. It couples the two kinds of damages, meaning that the transverse micro-cracking appearing inside the plies will influence the initiation of delamination at the interface of the plies. With this new model, delamination occurs earlier in terms load level, what is closer to what is observed in the physical tests.

In this paper, this new non local model is first described. Since it includes many parameters, a procedure for the parameter identification is discussed. A comparison of the solution obtained with the classical damage models and the new advanced formulation is then conducted.

KEYWORDS

Composite, damage, non-local approach, Cachan model

ADVANCES IN THE PROGRESSIVE DAMAGE ANALYSIS OF COMPOSITES

1: Intra-laminar damage modelling with SAMCEF

The damage model for an unidirectional ply is based on the work done at Cachan and presented in [1,2]. It is extended here to the general 3D case in (1) and is expressed in terms of the stresses. Three damage variables are taken into account. The first one, d_{11}, manages the damage in the fibre direction; the second one, d_{22}, collects the damage in the transverse direction (occurring only in traction), while d_{12} can handle the damage in the shear direction, reflecting the de-cohesion between the fibres and the matrix. When the plane stress assumption is not done, the damage can also occur in direction 3. The parameter λ, whose value is equal to 0 or 1, is then introduced.

$$\begin{aligned}E = &\frac{\sigma_{11}^2}{2(1-d_{11})E_1^0} - \frac{\nu_{12}^0}{E_1^0}\sigma_{11}\sigma_{22} - \frac{\nu_{13}^0}{E_1^0}\sigma_{11}\sigma_{33} + \frac{\langle\sigma_{22}\rangle_+^2}{2(1-d_{22})E_2^0} + \frac{\langle\sigma_{22}\rangle_-^2}{2E_2^0} \\ &+ \frac{\langle\sigma_{33}\rangle_+^2}{2(1-\lambda d_{22})E_3^0} + \frac{\langle\sigma_{33}\rangle_-^2}{2E_3^0} - \frac{\nu_{23}^0}{E_2^0}\sigma_{22}\sigma_{33} + \frac{\sigma_{12}^2}{2(1-d_{12})G_{12}^0} + \frac{\sigma_{13}^2}{2(1-\lambda d_{12})G_{13}^0} \\ &+ \frac{\sigma_{23}^2}{2(1-\lambda d_{22})G_{23}^0}\end{aligned} \qquad (1)$$

As the strains can be determined by the derivative of the potential (1) with respect to the stresses, the thermodynamic forces Y_i are computed as the derivatives of the potential with respect to the damage variables d_i. The damages increase as the corresponding thermodynamic force increases, as illustrated in Figure 1, where $Y = Y_{12} + b_2 Y_{22}$. It is also noted that $d_{22} = b_3 d_{12}$. As soon as either d_{12} or d_{22} is equal to 1, then d_{22} or d_{12}, respectively, is set to 1: once the ply is broken in the transverse direction because of too many cracks in the matrix, the resistance to shear vanishes; the opposite is also true.

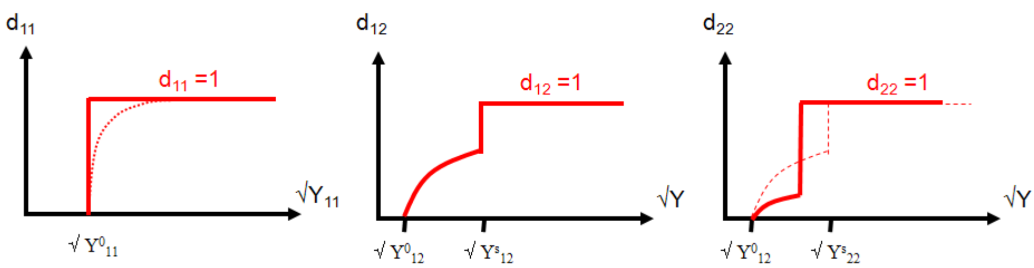

Figure 1: Evolution of the damages wrt the thermodynamic forces.

For modelling the damage, several parameters then have to be identified: Y^0_{12}, Y^s_{12}, the expression of the non-linear part of $d_{12}=d_{12}(\sqrt{Y})$, Y^s_{22}, Y^0_{11} (in traction and compression), b_2 and b_3. Besides the damage associated to the failure of the ply, permanent deformation is also observed, when the matrix is loaded (Figure 2). The equations are given in (2), and the parameters to identify are R_0, β, γ and a. Note that the effective stresses are used in the plasticity criterion.

$$f(\tilde{\sigma}, p) = \sqrt{\tilde{\sigma}_{12}^2 + \lambda(\tilde{\sigma}_{13}^2 + \tilde{\sigma}_{23}^2) + a^2(\tilde{\sigma}_{22}^2 + \tilde{\sigma}_{33}^2)} - R_0 - R(p) \leq 0$$

$$R(p) = R_0 + \beta p^{\gamma} \quad (2)$$

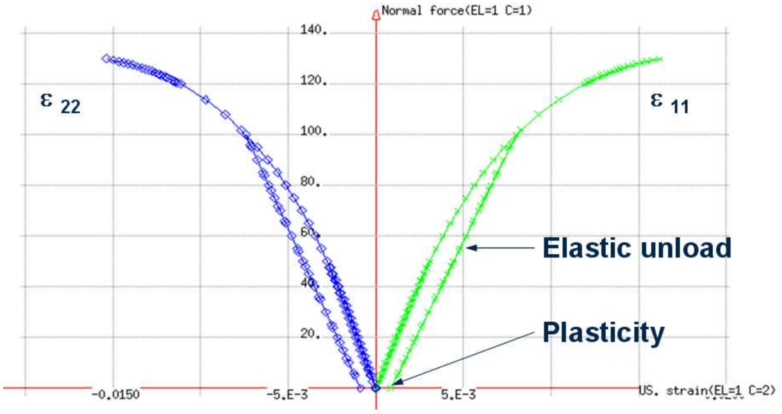

Figure 2: Permanent deformation in the matrix of a $[45/-45]_s$ laminate

As reported in [1], all these parameters, as well as the elastic constants, can be identified based on the tests results on three different laminates, that are coupons with 0/90, 45/-45 and 67.5/-67.5 stacking sequences. The test on the 0/90 allows to determine the properties in the fibre direction; the tests on the 45/-45 are used to identify the shear parameters, as well as the parameters for plasticity (except the parameter called *a*); finally, the tests results on the 67.5/-67.5 can provide the coupling coefficients.

2: Inter-laminar damage modelling with SAMCEF

Delamination is modelled in SAMCEF with the cohesive elements approach developed by Cachan, based on the work described in [3-5]. The implementation was described in [3-6], and is therefore not reported here in details. The cohesive elements approach has been used mainly for the study of stable crack propagation, to simulate either for DCB, ENF or MMB tests. Here, as an illustration of the SAMCEF capabilities, the unstable propagation on an ENF is presented (Figure 3). The initial crack length is such that an unstable path will appear during the crack propagation, what will result in a snap-back in the reaction/displacement equilibrium curve. This unstable path is captured thanks to a continuation approach in the solution of the non-linear equations; n this case the Riks method is used. Figure 4 shows the equilibrium path and the deformation of the ENF over time. It is clear that the crack propagates quite suddenly. This acceleration in the crack propagation leads to a sudden change in the geometry of the specimen. At that time, the snap-back occurs.

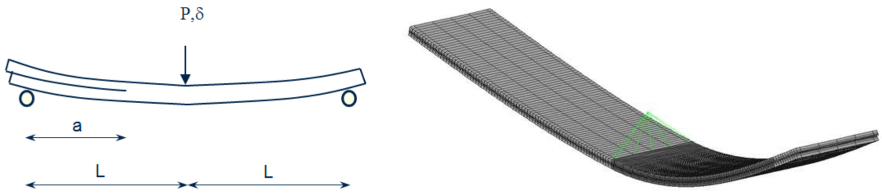

Figure 3: The ENF problem and the corresponding SAMCEF model

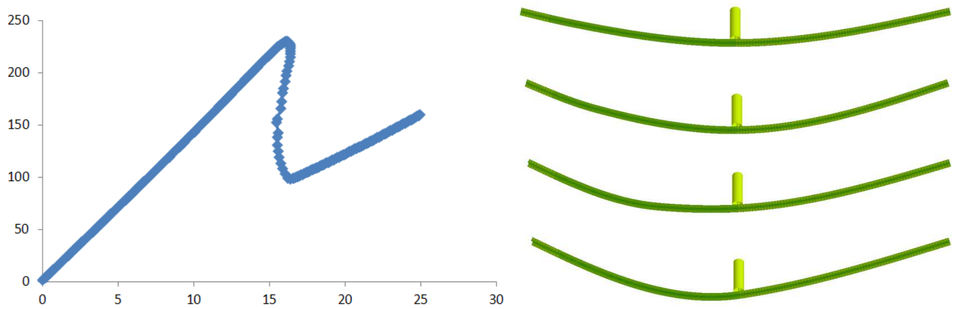

Figure 4: Results of the FE simulation

3: Non-local approach: coupling inter and intra-laminar damages

Based on the work done at Cachan and described in [7], a non-local approach has been implemented in SAMCEF. In this approach, the transverse cracking in the matrix will influence the resistance of the interface, and will therefore initiate the delamination.

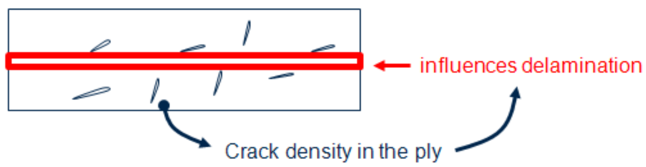

Figure 5: Effect of the transverse cracking on the interface strength

On one side, we have the diffuse damage, which is related to the evolution of the damage before the limiting value Y^s_{12} and Y^s_{22} are reached. On the other side, transverse micro-cracking also evolves through the ply thickness. Damages $\bar{d}_{22}$, $\bar{d}_{12}$ and $\bar{d}_{23}$ are associated to the micro-cracking density ρ (3). d_{23} depends on the damage d_{22} and on the Poisson coefficient ν_{23}. The stiffnesses are now degraded according to:

$$E_2 = E_2^0(1-d_{22})(1-\bar{d}_{22})$$

$$G_{12} = G_{12}^0(1-d_{12})(1-\bar{d}_{12})$$

$$G_{23} = G_{22}^0(1-d_{23})(1-\bar{d}_{23})$$

The value of ρ is obtained by solving equation (4).

$$\bar{d}_{22} = \bar{d}_{22}(\rho) \qquad \bar{d}_{12} = \bar{d}_{12}(\rho) \qquad \bar{d}_{23} = \bar{d}_{23}(\rho) \tag{3}$$

$$\left[\left(\frac{Y_{22}\dfrac{\partial \bar{d}_{22}}{\partial \rho}}{G_I^C(1-d_{22})}\right)^{\alpha} + \left(\frac{Y_{12}\dfrac{\partial \bar{d}_{12}}{\partial \rho}}{G_{II}^C(1-d_{12})}\right)^{\alpha} + \left(\frac{Y_{23}\dfrac{\partial \bar{d}_{23}}{\partial \rho}}{G_{III}^C(1-d_{23})}\right)^{\alpha}\right]^{1/\alpha} - 1 = 0 \tag{4}$$

Moreover, the value of the mean micro-cracking density $\bar{\rho}$ influences the strength of the interface in modes II and III, as expressed by (5) and (6). The damage d_I in the opening mode is obtained based on the corresponding thermodynamic force as in the uncoupled inter-laminar approach. For a micro-cracking density larger than a threshold ρ_s, the damage in the interface in modes II and III takes the value of d_I.

If $\rho < \rho_s$: $\quad d_{II} = d_I + (1-d_I)2a_i\bar{\rho}\sin^2\left(\frac{\theta}{2}\right)$ and $\quad d_{III} = d_I + (1-d_I)2a_i\bar{\rho}\cos^2\left(\frac{\theta}{2}\right)$ (5)

If $\rho \geq \rho_s$: $\quad d_{II} = d_I = 1$ and $\quad d_{III} = d_I = 1$ (6)

In practice , a delay effect avoids the numerical instabilities.

4: Illustration

The static indentation of a composite plates is considered. In Figure 6, the value of the damage at the interface of the plies when the uncoupled approach is used is given on the left. On the right, the damage values for delamination when the coupling between inter and intra-laminar models is taken into account. As expected, when the coupled model is used, the value of the inter-laminar damage is larger.

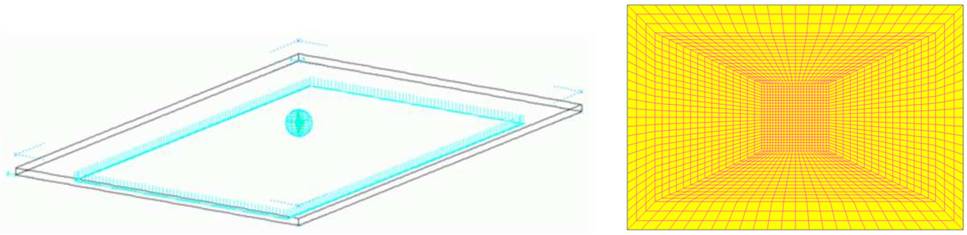

Figure 6: The static indentation problem and the SAMCEF FE model

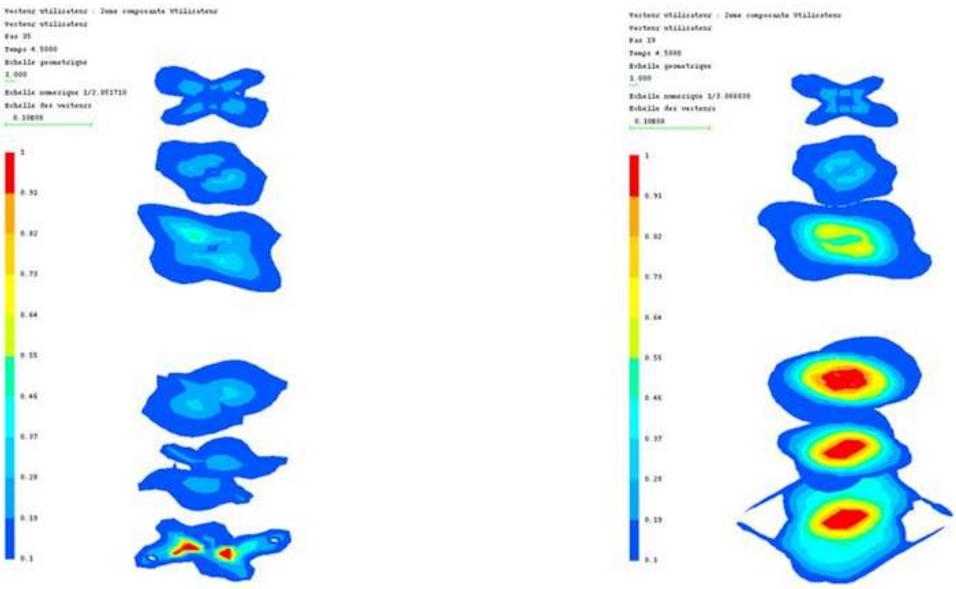

Figure 7: Inter-laminar damage with and without the coupling

5: Conclusions

In this paper, the damage models available in SAMCEF were recalled, and the parameters to identify were listed. A new non local model was described. This model makes a link between inter and intra-laminar damages. An application illustrates the accuracy of the models, when they are used in a coupled and uncoupled way.

REFERENCES

[1] Ladeveze P., and Le Dantec S. (1992). "Damage modeling of the elementary ply for laminated composites", Composites Science and Technology, 43, 1992.

[2] Ladevèze P. and Lubineau G. (2001). "On a damage mesomodel for laminates : micro-meso relationships, possibilities and limits". Composites Science and Technology, 61, pp. 2149–2158.

[3] Allix O. and Ladevèze P.(1992). "Interlaminar interface modelling for the prediction of laminate delamination", Composite Structures, 22:235-242

[4] Allix O., Lévêque D. and Perret L. (1998). "Interlaminar interface model identification and forecast of delamination in composite laminates". Comp. Sci. Techn. 56 :671-678.

[5] Ladevèze, P. et al. (1198). "A Computational Method for damage Intensity Prediction in a Laminated Composite Structure", Computational mechanics—New Trends and Applications In: Idelsohn, S., Oñate E., and Dvorkin E., (eds.) CIMNE, Barcelona, Spain (1998).

[6] Brauner C., Delsemme J.P. Jetteur Ph., Bruyneel M., and Kuhlmann G. (2009). "Non linear failure analysis of a reinforced composite curved beam with delamination and ply degradation", NAFEMS World Congress", 16-19 June 2009, Crete, Greece.

[7] Bruyneel M., Delsemme J.P., Jetteur P. and Remouchamps (2010). "SAMCEF for composites : advanced numerical methods for analysis and optimisation", NAFEMS Seminar "Simulating Composite Materials and Structures,2nd – 3rd February 2010, Esbjerg, Denmark.

[8] Bruyneel M., Delsemme J.P., Jetteur Ph. and Mertens T. (2011). "Recent results in damage modelling of composites", NAFEMS World Congress, May 23-26, 2011, Boston, USA.

[9] Bruyneel M., Delsemme J.P., Jetteur P., Germain F. (2009). "Modeling inter-laminar failure in composite structures: illustration on an industrial case study", Applied Composite Materials, 16(3), 149-162.

[10] Abisset E. (2012). "Un mésomodèle d'endommagement des composites stratifiés pour le virtual testing: identification et validation", PhD Thesis, ENS Cachan, France.

[11] Lubineau G. and Ladeveze P. (2008). "Construction of a micromechanics-based intralaminar model and illustrations in Abaqus standard", Computational Materials Science, 43(1), pp. 137-145.